

# MODELING THE NON-REVERSIBLE SERIES-RESONANT CONVERTER OPERATING IN ZERO VOLTAGE SWITCHING MODE

Patrick Kuo-Peng

Universidade Federal de Santa Catarina  
GRUCAD-EEL-CTC-UFSC-CNPQ/RHAE  
C.P. 476  
88040-900 -Florianópolis- SC  
Brasil

and

Yvon Chéron

LEEI / ENSEEIHT  
U.R.A. au C.N.R.S. n° 847  
2, rue Charles Camichel  
31071 Toulouse Cédex  
France

**Abstract** - This paper presents a steady state modeling of the non-reversible series-converter operating in Zero Voltage Switching (ZVS) mode. This modeling is based on the representation in the state plane of the converter steady state operation. This method enables a full characterization of the converter. The studied structure is composed of a full bridge inverter and a full bridge rectifier. It can be equipped with snubbers. The modeling method presented can also be applied to the variants of the basic one. Moreover, the analytical work is based on normalized quantities which lead to the derivation of dimensionless equations that characterize a structure instead of a particular circuit. The results of these analytical studies are integrated into a software which constitutes a powerful tool to design the converter.

## NOMENCLATURE

|                 |   |
|-----------------|---|
| L               | Resonant inductor.  |
| C               | Resonant capacitor.   |
| C <sub>1j</sub> | Snubber capacitor of the inverter.  |
| C <sub>2j</sub> | Snubber capacitor of the rectifier.   |
| C <sub>1</sub>  | Capacitor representing the snubber of the inverter during its commutation.  |
| C <sub>2</sub>  | Capacitor representing the snubber of the rectifier during its commutation. |
| f <sub>0</sub>  | Natural frequency of the resonant circuit.                                  |
| f               | Frequency of operation.   |
| E <sub>1</sub>  | Input voltage.  |
| E <sub>2</sub>  | Output voltage.   |
| j               | Current in the resonant circuit.  |
| I <sub>2</sub>  | Output average current.   |
| V <sub>c</sub>  | Voltage across the resonant capacitor.                                      |
| k               | Turns ratio of the transformer.   |

In addition to these notations, the various analytic studies of the series-resonant converter exposed in this paper use the following normalized units :

$$y = \frac{j}{E_1 \sqrt{\frac{C}{L}}} \quad \text{Normalized current in the resonant tank.}$$

$$y_{\text{avg}} = \frac{k I_2}{E_1 \sqrt{\frac{C}{L}}} \quad \text{Normalized average load current.}$$

$$X = \frac{V_c}{E_1} \quad \text{Normalized voltage across capacitor C.}$$

$$X_m = \frac{V_{\text{cmax}}}{E_1} \quad \text{Normalized maximum voltage across C.}$$

$$q = \frac{E_2}{k E_1} \quad \text{Normalized load voltage.}$$

$$u = \frac{f}{f_0} \quad \text{Normalized frequency of operation.}$$

$$a_1 = \frac{C_1}{C} \quad \text{Normalized snubber capacitor of the inverter.}$$

$$a_2 = \frac{k^2 C_2}{C} \quad \text{Normalized snubber capacitor of the rectifier.}$$

In this paper, function  $\text{Atan2}(x)$  is the function  $\text{Arctg}(x)$  with value lying between 0 and  $\pi$ .

## I. INTRODUCTION

Due to their numerous advantages, viz., higher frequency of operation, reduced size and weight, reduction of the component stresses, etc..., series-resonant converters are widely used. Despite this, there are not many studies or scientific papers about their modeling, particularly when their snubbers are taken into account both in the inverter side and in the rectifier side. The authors first define the assumptions and the studying method. Based on the state plane representation, this method leads to a full characterization of the converter steady state operation (DC output voltage versus load average current at constant frequency, peak current in the switches versus average load current at constant output voltage ...). This characterization gives an overview of the converter steady state operation. The analysis of these characteristics enables to carry out a method to design the converter.

## II. ASSUMPTIONS

The study of the converter is carried out under the following assumptions :

- the transformer is ideal and has a 1:1 ratio,
- the switches are ideal in that they commute instantaneously,
- the input and output DC voltage are perfectly smooth within the period of the converter operation,
- the losses in the resonant circuit are negligible.

## III. PRESENTATION OF THE NON-REVERSIBLE SERIES-RESONANT CONVERTER OPERATING IN ZVS MODE

The series-resonant converters are indirect DC/DC converters with intermediate high-frequency link. They are mainly composed of a voltage inverter and a current rectifier connected through a series-resonant circuit and a transformer (Fig. 1).

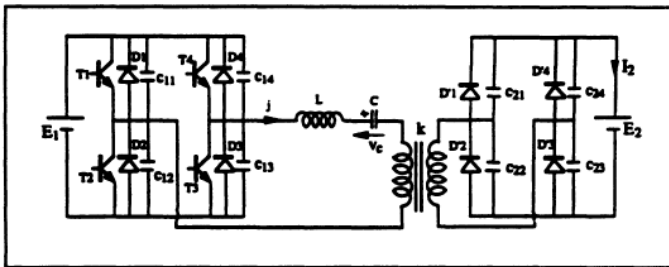


Fig. 1: Structure of the converter.

The non-reversibility of the structure is imposed by the diode rectifier. On the inverter side, operation above natural frequency of the resonant circuit requires turn-off controlled and spontaneous turn-on switches. The Dual-Thyristor corresponds to this mode of operation. This kind of switch is not available as a component. It can be synthesized, for example, by a power transistor and a diode connected in anti-parallel [1]. In order to reduce the switches commutation losses, snubbers are added to the circuit. At the rectifier side, these snubbers are represented whether by capacitors added in parallel with each diode, whether by parasitic capacitance of the transformer secondary windings. At the inverter side, due to the turn-off control of the dual-thyristor, it is necessary to limit the voltage variation across its terminals ( $dv/dt$ ). The snubber of this switch can be capacitors. Owing to the fact that the dual-thyristor commutates at the voltage zero crossing, no energy is stored in these snubbers. Therefore, they are not dissipative and can be overdimensionned.

## IV. MODELING THE CONVERTER

### IV.1 Studying method

According to the assumptions above and when the snubbers are neglected, the study of the series-resonant converter reduces, at each sequence of its operation, to the

study of the response of a series-resonant tank connected on one side to a voltage source  $v_1 = \pm E_1$  of frequency  $f$  and on the other side to a voltage source  $v_2 = \pm E_2$ , in phase with the current in the resonant circuit (Fig. 2) [2].

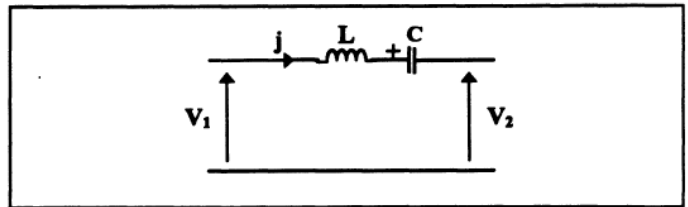


Fig. 2: method of study.

The study of the converter is greatly facilitated by using the state plane representation of these equivalent circuits. As a matter of fact, it avoids writing time equations of the system, which are very cumbersome to use. However, taking the snubbers of the converter into account lead to characterize three modes of operation :

- Normal operation, in which the dual-thyristors turn-off control are made after the end of the rectifier commutation (Fig. 3). The latter occurs when the capacitor  $C_2$  representing the snubber of the rectifier during its commutation is reverse biased.

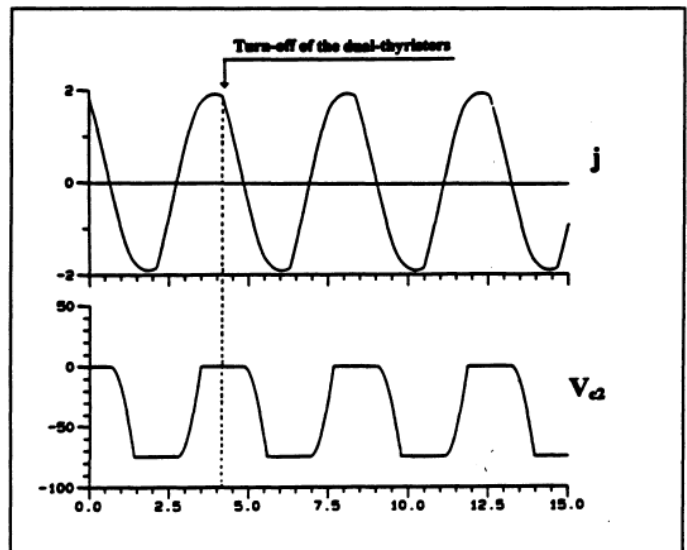


Fig. 3: Wave-forms of the converter in normal operation.

- Secondary operation, characterized by the fact that the dual-thyristors turn-off control are made before the end of the rectifier commutation (Fig. 4). No-load operation is a particular case of the secondary operation.

- Criss-cross operation, in which the rectifier commutation ends during the inverter commutation. This operation is impossible to be solved analytically. Nevertheless, the criss-cross operation area is negligible in comparison with the both other operations. A linear interpolation on the limit of these operations enables a full characterization of the converter.

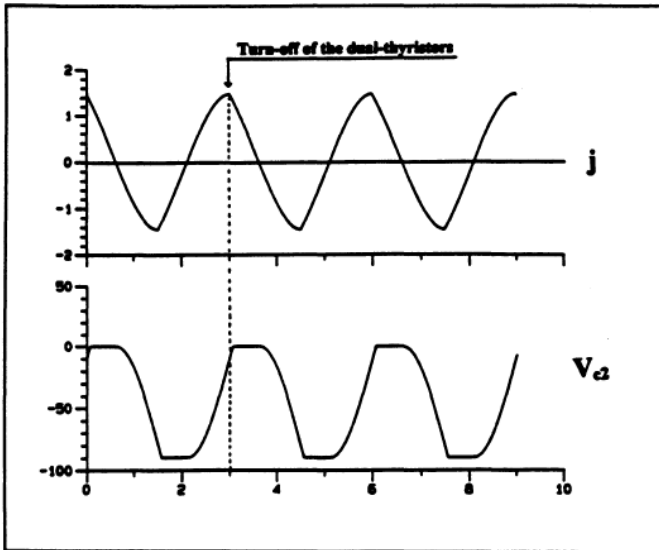


Fig. 4: Wave-forms of the converter in secondary operation.

Consequently, the study of the converter is no more limited by the study of the simplified circuit presented in Fig.2. It must be included the snubbers. That leads to analyze, at each sequence of operation, equivalent circuits with different pulsations. Thus, in order to carry out this study, several state planes should be used : one to show the operation between commutation and the others to represent the commutations. Nevertheless, it will be shown that it is possible to determine appropriate formula allowing transition from one state plane to the other one.

In this paper, owing to the symmetry of the converter operation, only the positive half-wave of the current is represented in the state plane.

#### IV.2 State plane representation and analysis

The structure of the converter to be studied is indicated in Fig.1. Let :

$$C_1 = (C_{11} + C_{14}) // (C_{12} + C_{13}) \quad (1)$$

$$C_2 = (C_{21} + C_{24}) // (C_{22} + C_{23}) \quad (2)$$

$$k_1^2 = 1 + \frac{1}{a_1} \quad (3)$$

$$k_2^2 = 1 + \frac{1}{a_2} \quad (4)$$

$$G_1 = \frac{C_1 C}{C_1 + C} \quad (5)$$

$$G_2 = \frac{C_2 C}{C_2 + C} \quad (6)$$

##### IV.2.a Normal operation

**Representation in the state plane.** The normal operation is characterized by the series of modes indicated in Fig.5 and the corresponding wave-forms are presented in Fig.3.

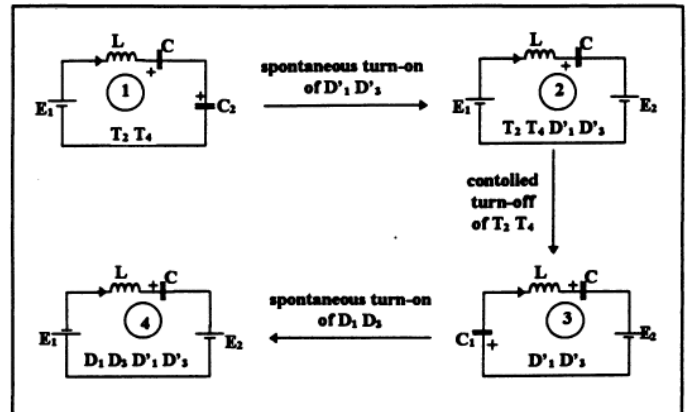


Fig. 5: Sequence of modes in normal operation.

Mode 1 represents the rectifier commutation. It is initiated by the current zero crossing in the resonant circuit. This mode takes end when the capacitor  $C_2$  is reverse biased (mode 2). Mode 3 corresponds to the inverter commutation and it is initiated by the control signal. This mode ends when the capacitor  $C_1$  is reverse biased (mode 4). Note that the pulsation of the alternative quantities is equal to

$$\omega^* = \frac{1}{\sqrt{L G_2}} \text{ during the rectifier commutation (mode 1),}$$

$$\omega^0 = \frac{1}{\sqrt{L G_1}} \text{ during the inverter commutation (mode 3) and}$$

$$\omega = \frac{1}{\sqrt{LC}} \text{ between the commutations (modes 2 and 4).}$$

Consequently, the normal operation must be drawn in three different state planes (Fig. 6).

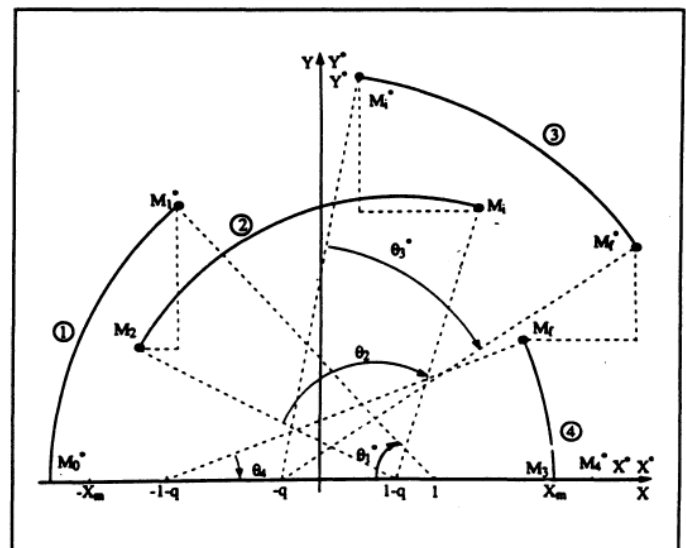


Fig. 6: State plane representation. Normal operation.

$X_j$  and  $Y_j$  are the coordinates of  $M_j$  ( $j = 2, 3, i$  or  $f$ ).

$X_j^*$  and  $Y_j^*$  are the coordinates of  $M_j^*$  ( $j = 0, 1$  or  $4$ ).

$X_j^0$  and  $Y_j^0$  are the coordinates of  $M_j^0$  ( $j = i$  or  $f$ ).

Otherwise, let :

$$X^0 = \frac{V_{G1}}{E_1} \quad (7)$$

$$Y^0 = \frac{j}{E_1} \sqrt{\frac{L}{G_1}} \quad (8)$$

$$X^* = \frac{V_{G2}}{E_1} \quad (9)$$

$$Y^* = \frac{j}{E_1} \sqrt{\frac{L}{G_2}} \quad (10)$$

where  $G_1$  and  $G_2$  are respectively voltage across capacitors  $C_1$  and  $C$  connected in series and voltage across capacitors  $C_2$  and  $C$  connected in series.

$\theta_1^*$  and  $\theta_2$  correspond to the normalized conduction times of the inverter transistors;  $\theta_4$  that of the inverter diodes.  $\theta_1^*$  and  $\theta_3^0$  are respectively the normalized commutation times of the rectifier and of the inverter.

The transformation rules allowing transition from the state plane  $(X, Y)$  to the state plane  $(X^*, Y^*)$  are given by the following equations :

- before the rectifier commutation

$$X^* = X - q \quad (11)$$

$$Y^* = k_2 Y \quad (12)$$

- after the rectifier commutation

$$X^* = X + q \quad (13)$$

$$Y^* = k_2 Y \quad (14)$$

and those between the state plane  $(X, Y)$  and the state plane  $(X^0, Y^0)$  are given by :

- before the inverter commutation

$$X^0 = X - 1 \quad (15)$$

$$Y^0 = k_1 Y \quad (16)$$

- after the inverter commutation

$$X^0 = X + 1 \quad (17)$$

$$Y^0 = k_1 Y \quad (18)$$

**State plane analysis.** The key relationships that fully determine the state plane trajectories are :

$$(X_0^* - 1)^2 = (X_1^* - 1)^2 + Y_1^{*2} \quad (19)$$

$$(X_2 - 1 + q)^2 + Y_2^2 = (X_i - 1 + q)^2 + Y_i^2 \quad (20)$$

$$(X_i^0 + q)^2 + Y_i^{02} = (X_f^0 + q)^2 + Y_f^{02} \quad (21)$$

$$(X_f + 1 + q)^2 + Y_f^2 = (X_3 + 1 + q)^2 \quad (22)$$

According to relation (13) and knowing that  $X_3 = X_m$  :

$$X_4^* = X_m + q \quad (23)$$

The voltage variation across the equivalent capacitor  $G_1$  during the inverter commutation is given by :

$$X_f^0 - X_i^0 = 2(1 + a_1) \quad (24)$$

or

$$X_f - X_i = 2 a_1 \quad (25)$$

and that of the equivalent capacitor  $G_2$  during the rectifier commutation is given by :

$$X_1^* - X_0^* = 2q(1 + a_2) \quad (26)$$

Finally, from relations (11) to (26), it is possible to determine entirely the coordinates of the state plane in the normal operation in terms of  $q, X_m, a_1$  and  $a_2$  :

$$X_0^* = -X_m - q \quad (27)$$

$$X_1^* = -X_m + q + 2q a_2 \quad (28)$$

$$Y_1^{*2} = 4q(X_m + 1 - q a_2)(1 + a_2) \quad (29)$$

$$X_2 = 2q a_2 - X_m \quad (30)$$

$$Y_2^2 = 4q a_2 (X_m + 1 - q a_2) \quad (31)$$

$$X_i = q X_m - q^2 a_2 - a_1 \quad (32)$$

$$Y_i^2 = (X_2 - 1 + q)^2 + Y_2^2 - (X_i - 1 + q)^2 \quad (33)$$

$$X_i^0 = q X_m - a_2 q^2 - a_1 - 1 \quad (34)$$

$$Y_i^0 = k_1 Y_i \quad (35)$$

$$X_f = q X_m - q^2 a_2 + a_1 \quad (36)$$

$$Y_f^2 = (X_m + X_f + 2 + q)(X_m - X_f) \quad (37)$$

$$X_f^0 = q X_m - q^2 a_2 + a_1 + 1 \quad (38)$$

$$Y_f^0 = k_1 Y_f \quad (39)$$

Mathematical relations (27) to (39) enable to characterize the normal operation of the converter. However, it is necessary to define their application range corresponding to the sequence of modes shown in Fig. 5. Thus, the following equations must be verified :

$$X_i > X_2 \quad (40)$$

$$X_3 > X_f \quad (41)$$

These relations mean respectively that the dual-thyristors turn-off control are made only after the end of rectifier commutation and that the inverter commutation ends at zero current crossing in the resonant circuit.

The area of the normal operation is determined in the plane  $q(X_m)$  (Fig. 9a to Fig. 9c) by the boundaries locus defined by :

$$X_i = X_2 \quad (42)$$

$$X_3 = X_f \quad (43)$$

or in terms of  $q, X_m, a_1$  and  $a_2$  :

$$X_m = \frac{2q a_2 + q^2 a_2 + a_1}{1 + q} \quad (44)$$

$$X_m = \frac{a_1 - q^2 a_2}{1 - q} \quad (45)$$

The normalized frequency of operation is given by :

$$u = \frac{\pi}{\frac{\theta_1^*}{k_2} + \theta_2 + \frac{\theta_3^0}{k_1} + \theta_4} \quad (46)$$

where

$$\theta_1^* = \pi - A \tan 2 \left( \frac{Y_1^*}{X_1^* - 1} \right) \quad (47)$$

$$\theta_2 = A \tan 2 \left( \frac{Y_2}{X_2 - 1 + q} \right) - A \tan 2 \left( \frac{Y_i}{X_i - 1 + q} \right) \quad (48)$$

$$\theta_3^0 = A \tan 2 \left( \frac{Y_i^0}{X_i^0 + q} \right) - A \tan 2 \left( \frac{Y_f^0}{X_f^0 + q} \right) \quad (49)$$

$$\theta_4 = A \tan 2 \left( \frac{Y_f}{X_f + 1 + q} \right) \quad (50)$$

The normalized average load current is given by :

$$Y_{avg} = \frac{2u(X_m - a_2 q)}{\pi} \quad (51)$$

The normalized peak current in the resonant circuit, thus in the switches, is equal to :

$$Y_{max} = X_m + 1 + q \quad \text{if } X_f < -1 - q \quad (52)$$

$$Y_{max} = \sqrt{(X_i - 1 + q)^2 + Y_i^2} \quad \text{if } (X_f > -1 - q) \text{ and } (X_i > 1 - q) \quad (53)$$

$$Y_{max} = Y_i \text{ or } Y_f \quad \text{if } (X_f > -1 - q) \text{ and } (X_i < 1 - q) \quad (54)$$

$$Y_{max} = Y_2 \quad \text{if } X_2 > 1 - q \quad (55)$$

The normalized current in the resonant circuit or in the switches at the turn-off time of the transistors is given by :

$$Y_{cbl} = \sqrt{(X_2 - 1 + q)^2 + Y_2^2 - (X_i - 1 + q)^2} \quad (56)$$

#### IV.2.b Secondary operation

**Representation in the state plane.** The secondary operation is represented by the sequence of modes indicated in Fig. 7. This operation can be shown up by the analysis of the current wave-form in the resonant circuit and of the voltage wave-form across the rectifier snubber capacitor (Fig.4).

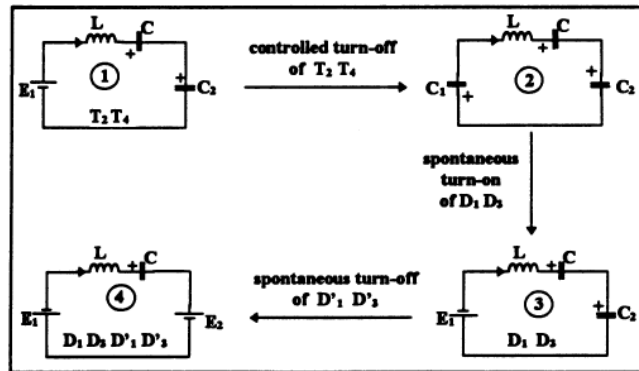


Fig. 7: Sequence of modes in secondary operation.

When the dual-thyristors are triggered before the end of the rectifier commutation, no switch neither of the inverter, nor of the rectifier is conducting. So, the current in the resonant circuit conducts to the snubber capacitors both of the inverter and of the rectifier.

In the light of remarks made in the foregoing paragraph, the secondary operation can be drawn in the state plane (Fig. 8).

$X^*$  and  $Y^*$  are always equal respectively to the relations (9) and (10). Otherwise, let :

$$k_{12}^2 = 1 + \frac{1}{a_1 k_2^2} \quad (57)$$

$$G_{12} = \frac{C C_1 C_2}{C C_1 + C C_2 + C_1 C_2} \quad (58)$$

$$X^0 = \frac{V_{G12}}{E_1} \quad (59)$$

$$Y^0 = \frac{j}{E_1} \sqrt{\frac{L}{G_{12}}} \quad (60)$$

Where  $G_{12}$  is the equivalent capacitor representing the capacitors  $C$ ,  $C_1$  and  $C_2$  connected in series.

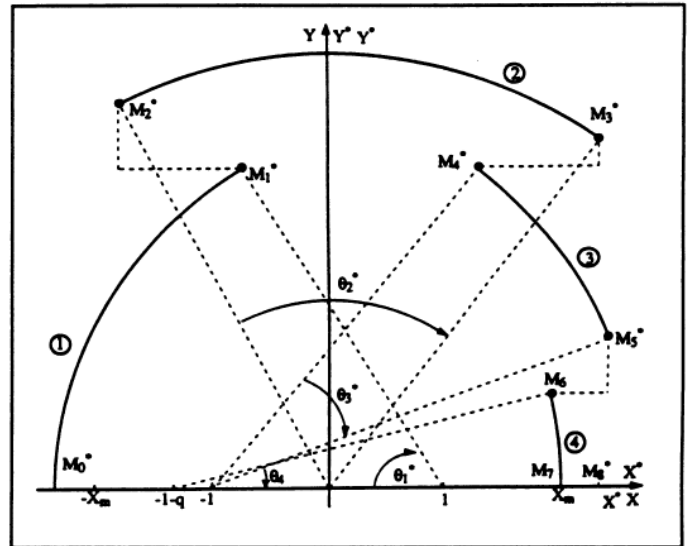


Fig. 8: State plane representation. Secondary operation.

$\theta_1^*$  is the transistor conduction angle;  $\theta_3^*$  and  $\theta_4$  those of the inverter diodes.

$\theta_1^*$ ,  $\theta_2^*$  and  $\theta_3^*$  are the rectifier commutation angles;  $\theta_2^0$  that of the inverter.

The transformation rules allowing transition from state plane  $(X, Y)$  to state plane  $(X^*, Y^*)$  are still given by relations (11) to (14), and those between state plane  $(X^*, Y^*)$  and state plane  $(X^0, Y^0)$  are given by :

- before the inverter commutation

$$X^0 = X^* - 1 \quad (61)$$

$$Y^0 = k_{12} Y^* \quad (62)$$

- after the inverter commutation

$$X^0 = X^* + 1 \quad (63)$$

$$Y^0 = k_{12} Y^* \quad (64)$$

**State plane analysis.** The main relations that enable us to determine the whole trajectory in the state plane are :

$$(X_0^* - 1)^2 = (X_1^* - 1)^2 + Y_1^{*2} \quad (65)$$

$$X_2^{*2} + Y_2^{*2} = X_3^{*2} + Y_3^{*2} \quad (66)$$

$$(X_4^* + 1)^2 + Y_4^{*2} = (X_5^* + 1)^2 + Y_5^{*2} \quad (67)$$

$$(X_6^* + 1 + q)^2 + Y_6^{*2} = (X_7^* + 1 + q)^2 \quad (68)$$

The voltage variation across the equivalent capacitor  $G_1$  during the inverter commutation is given by :

$$X_4^* - X_1^* = 2 a_1 k_2^2 \quad (69)$$

The voltage variation across the equivalent capacitor  $G_2$  during the rectifier commutation is given by :

$$X_5^* - X_0^* = 2q(1 + a_2) \quad (70)$$

Relations (11) to (14) and (61) to (70) enable to write all the coordinates of the state plane in the secondary operation in function of  $q$ ,  $X_m$ ,  $a_1$  and  $a_2$  :

$$X_0^* = -X_m - q \quad (71)$$

$$X_1^* = \frac{(X_m - a_2 q)(1 + q + a_2 q)}{a_2} - a_1 k_2^2 \quad (72)$$

$$Y_1^{*2} = (X_0^* + X_1^* - 2)(X_0^* - X_1^*) \quad (73)$$

$$X_2^{*0} = \frac{(X_m - a_2 q)(1 + q + a_2 q)}{a_2} - a_1 k_2^2 - 1 \quad (74)$$

$$Y_2^{*0} = k_{12} Y_1^* \quad (75)$$

$$X_3^{*0} = \frac{(X_m - a_2 q)(1 + q + a_2 q)}{a_2} + a_1 k_2^2 + 1 \quad (76)$$

$$Y_3^{*02} = X_2^{*02} + Y_2^{*02} - X_3^{*02} \quad (77)$$

$$X_4^* = \frac{(X_m - a_2 q)(1 + q + a_2 q)}{a_2} + a_1 k_2^2 \quad (78)$$

$$Y_4^* = \frac{Y_3^{*0}}{k_{12}} \quad (79)$$

$$X_5^* = -X_m + q(1 + 2 a_2) \quad (80)$$

$$Y_5^{*2} = 4 k_2 (q a_2 + q + 1)(X_m - q a_2) \quad (81)$$

$$X_6 = -X_m + 2q a_2 \quad (82)$$

$$Y_6^{*2} = 4(q a_2 + q + 1)(X_m - q a_2) \quad (83)$$

As for the normal operation, the application field of the mathematical relations above-stated must be defined and therefore, the following relations must be checked :

$$X_5^* > X_4^* \quad (84)$$

$$X_7 > X_6 \quad (85)$$

Relations (84) and (85) mean respectively that the dual-thyristors turn-off control are made before the end of the rectifier commutation and that the rectifier conducts current. The equality of relation (85) reflects the no-load operation of the converter. The limit loci associated with equations (84) and (85) are respectively defined by :

$$X_m = \frac{2q a_2 + q^2 a_2 - a_1}{1 + q} \quad (86)$$

$$X_m = q a_2 \quad (87)$$

An example of these boundaries locus is drawn in the plane  $q(X_m)$  (Fig. 9a to Fig. 9c)

The normalized frequency of operation is defined by :

$$u = \frac{\pi}{\frac{\theta_1^*}{k_2} + \frac{\theta_2^{*0}}{k_0} + \frac{\theta_3^*}{k_2} + \theta_4} \quad (88)$$

where

$$k_0 = \sqrt{1 + \frac{1}{a_1} + \frac{1}{a_2}} \quad (89)$$

$$\theta_1^* = \pi - A \tan 2 \left( \frac{Y_1^*}{X_1^* - 1} \right) \quad (90)$$

$$\theta_2^{*0} = A \tan 2 \left( \frac{Y_2^{*0}}{X_2^{*0}} \right) - A \tan 2 \left( \frac{Y_3^{*0}}{X_3^{*0}} \right) \quad (91)$$

$$\theta_3^* = A \tan 2 \left( \frac{Y_4^*}{X_4^* + 1} \right) - A \tan 2 \left( \frac{Y_5^*}{X_5^* + 1} \right) \quad (92)$$

$$\theta_4 = A \tan 2 \left( \frac{Y_6}{X_6 + 1 + q} \right) \quad (93)$$

The expression of the normalized average load current is always given by relation (51).

The normalized peak current in the resonant circuit, thus in the switches, is equal to :

$$Y_{\max} = \frac{1}{k_2} (X_m + q + 1) \text{ if } X_1^* > 1 \quad (94)$$

$$Y_{\max} = \frac{1}{k_0} (\sqrt{X_2^{*02} + Y_2^{*02}}) \text{ if } X_1^* < 1 \text{ and } X_3^{*0} > 0 \quad (95)$$

$$Y_{\max} = \frac{1}{k_2} (\sqrt{(X_4^* + 1)^2 + Y_4^{*2}}) \text{ if } X_1^* < 1 \text{ and } X_3^{*0} < 0 \quad (96)$$

The normalized current in the resonant circuit at the turn-off of the dual-thyristors is equal to :

$$Y_{\text{cbl}} = \frac{1}{k_2} (X_0^* + X_1^* - 2)(X_0^* - X_1^*) \quad (97)$$

## V. STATIC CHARACTERISTICS OF THE CONVERTER

These static characteristics are derived from steady state analytic study of the converter, using the normalized units and the assumptions defined above. These characteristics are very important since they are a powerful tool in analyzing the converter operation. In effect, they allow to determine the frequency range, and thus the power range attainable with a certain control range. They also show whether limiting the control range, limits the output current, and whether protection circuits are required. Plotting these characteristics is thus necessary to the design approach of the series-resonant converters.

### V.1 Plotting characteristics $q(X_m)$

These characteristics enable to discern the converter operating area. Regions (1), (2) and (3) of Fig. 9.a to Fig. 9.c correspond respectively to the region where the converter is

is working in the normal operation, secondary operation and criss-cross operation.

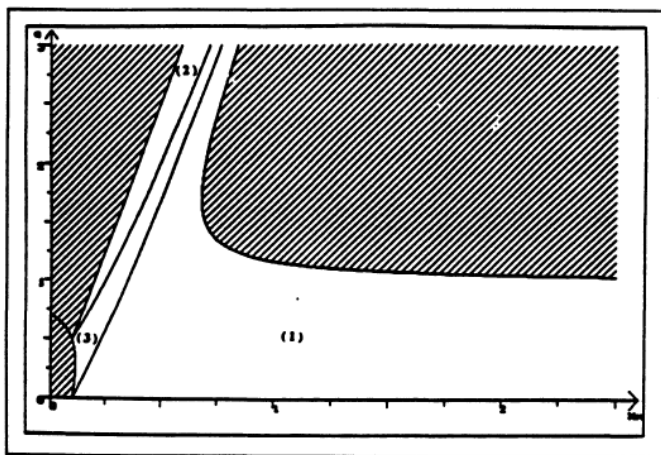


Fig. 9.a: Boundaries of the converter operation.  $a_1 < a_2$ .

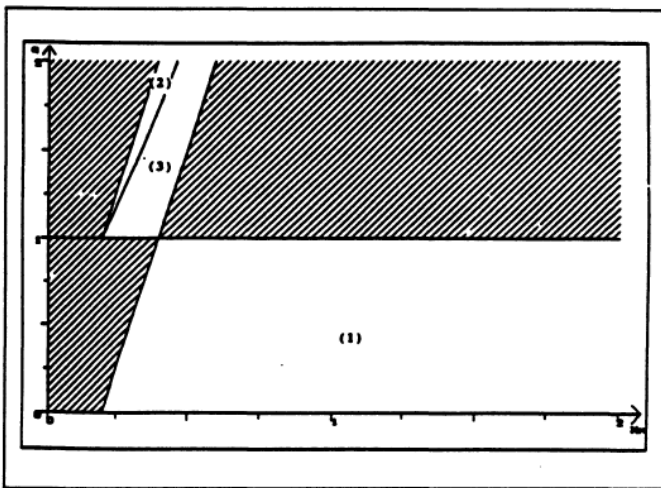


Fig. 9.b: Boundaries of the converter operation.  $a_1 = a_2$ .

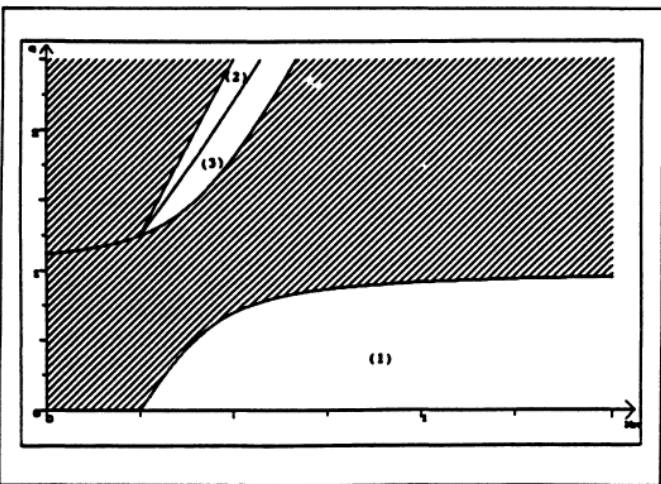


Fig. 9.c: Boundaries of the converter operation.  $a_1 > a_2$ .

When  $a_1 < a_2$  (Fig. 9.a), the converter operation is drawn in a single region limited by the  $X_m$  axis representing short-circuit operation, the line defined by relation (87)

representing no-load operation and the boundaries limit of the inverter commutation (relation 86).

When  $a_1 = a_2$  (Fig. 9.b) or  $a_1 > a_2$  (Fig. 9.c), the normal operation (region 1) is limited by the boundaries limit of inverter commutation (relation 86) and the  $X_m$  axis representing short-circuit operation. No-load operation is not possible in these cases. Regions (2) and (3) are not interesting because they require pre-established charging rate.

### V.2 Plotting the output characteristics of the converter

If the snubbers are neglected ( $a_1 = 0$  and  $a_2 = 0$ ), these characteristics are ellipses (Fig. 10.a). The snubbers of the inverter ( $a_1 > 0$  and  $a_2 = 0$ ) do not modify the shape of these characteristics but induce a commutation limit that prevents no-load operation (Fig. 10.b). In this region, the commutation failure leads to a stop of the inverter rather than its destruction.

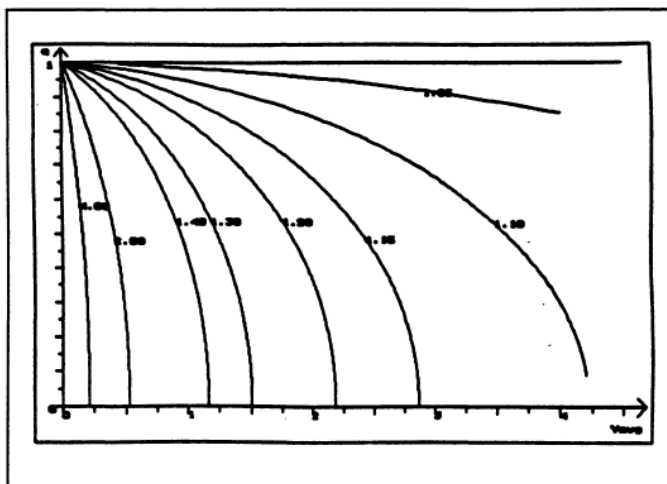


Fig. 10.a: Characteristics  $q(Y_{avg})$  at fixed  $u$ .  $a_1=0$  and  $a_2=0$ .

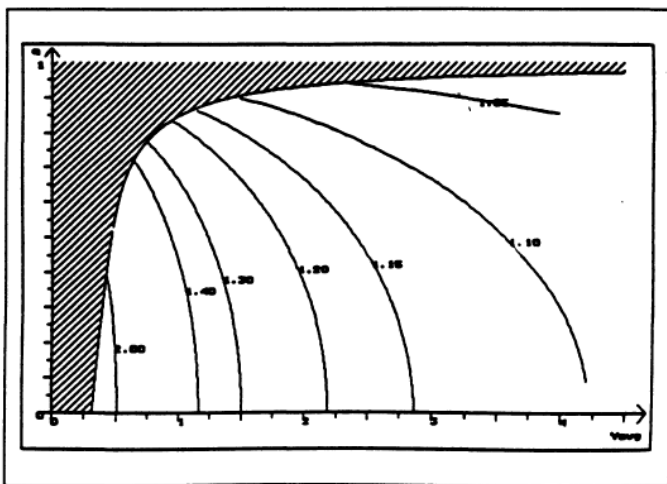


Fig. 10.b: Characteristics  $q(Y_{avg})$  at fixed  $u$ .  $a_1>0$  and  $a_2=0$ .

However, including the capacitive snubbers of the rectifier and especially when its value is greater than the inverter one ( $a_2 > a_1$ ), allow no-load operation (Fig. 10.c).

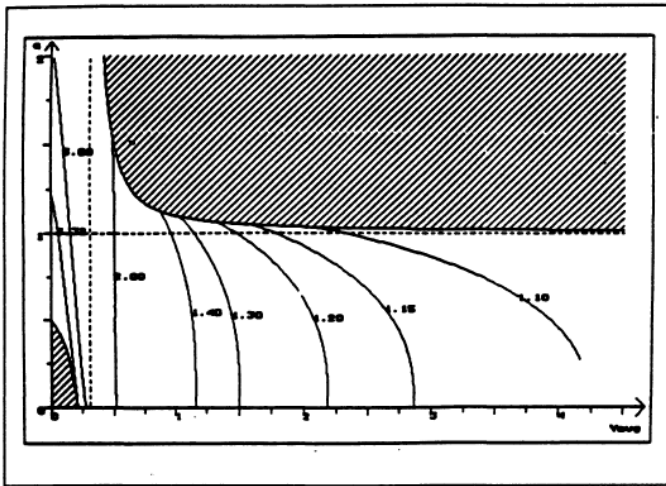


Fig. 10.c: Characteristics  $q(Y_{avg})$  at fixed  $u$ .  $a_2 > a_1$ .

### V.3 Plotting characteristics $G(H)$ with fixed $q$

These curves represent the evolution of an electric quantity ( $G$ ) versus a second one ( $H$ ) at a constant output voltage. These electric quantities can be :

- the average load current ( $Y_{avg}$ ),
- the frequency of operation ( $u$ ),
- the maximum voltage across the resonant capacitor ( $X_m$ ),
- the peak current in the resonant tank, thus in the switches ( $Y_{max}$ ),
- the current in the resonant circuit at the dual-thyristors turn-off ( $Y_{cb}$ ),
- the dual-thyristors delay angle, that is to say the angle between the current zero crossing in the resonant circuit and the dual-thyristors turn-off time ( $\omega t_{db} / \pi$ ).

These quantities are not exhaustive, because they are all accessible from the analysis of the state plane. An example of these characteristics is shown in Fig. 11. It represents the characteristic peak current in the switches ( $Y_{max}$ ) versus average load current ( $Y_{avg}$ ) at fixed output voltage ( $q$ ). The analysis of these characteristics enables to determine the current rating of the converter switches, thus their design.

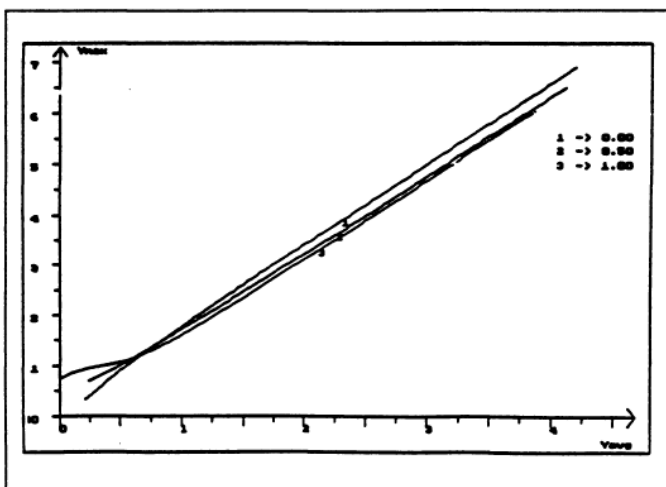


Fig. 11: Characteristics  $Y_{max}(Y_{avg})$  at fixed  $q$ .

## VI. CONCLUSION

The analytical study presented in this paper shows that the non-reversible series resonant converter operating in ZVS mode has some characteristics that depend strongly on the value of the snubbers. Thereby, this plotting characteristics software arised from the analytical study constitutes a good tool in analyzing the converter operation. Thus, the analysis of these characteristics enables also to carry out a method to design the converter.

## REFERENCES

- [1] H. Foch and J. Roux, "Convertisseurs statiques d'énergie électrique à semi-conducteurs", Brevet ANVAR, France n° 7832428, R.F.A. n° P29452457, G.B. n° 7939217, U.S.A. n° 093106, Italie n° 83487A/79.
- [2] R. Oruganty and F.C. Lee, "Resonant power processors : Part I - State plane analysis", *IEEE Trans. on Aerospace and Electronic Systems*, pp. 860-868, 1984.
- [3] V. Vorpérian and S. Cük, "A complete analysis of series-resonant converter", *IEEE Trans. on Industry Applications*, pp. 640-647, 1984.
- [4] P. Kuo-Peng, Y. Chéron, Ph. Cussac, "Program for the computer aided-design of the non reversible series-resonant converter operating above natural frequency", *EPE'91 Firenze*, vol. 4, pp. 231-236, September 1991.
- [5] Y. Chéron, "Soft commutation", *Chapman & Hall*, London 1992.
- [6] C. Q. Lee and K. Siri, "Analysis and design of series-resonant converter by state diagram", *IEEE Trans. on Aerospace and Electronic Systems*, pp. 537-544, 1986.
- [7] P. Kuo-Peng, "Conception assistée par ordinateur des convertisseurs à résonance série non réversible", *Thèse de Doctorat de l'INP Toulouse*, September 1993.

## CONTRIBUTORS

P. Kuo-Peng was born in Toamasina (Madagascar) in 1966. He received the Dr. degree in power electronics from the "Institut National Polytechnique de Toulouse", France in 1993. Since 1994, he has been with the department of electrical engineering of the federal University of Santa Catarina, Brazil, as an associate researcher in a research group called GRUCAD. He specializes in the modeling of static converters associated with two-dimensional finite element analysis of electrical machines. He is a member of Sbmag society.

Y. Chéron received the Docteur ès Sciences degree from the "Institut National Polytechnique de Toulouse", France. He is presently Directeur de Recherche at the CNRS. He has published more than 80 scientific papers on structures of static converters, resonant converter, soft commutation. He is also an author of a book about soft commutation.